CASL-U-2016-1052-000

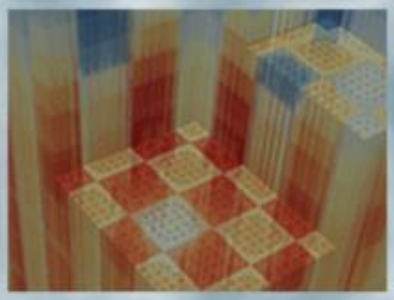

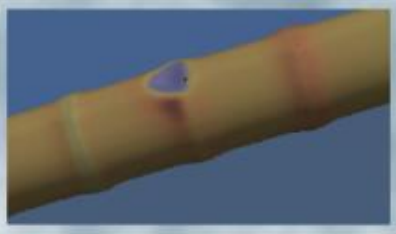

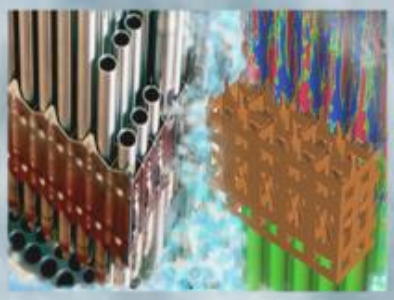

MPACT Library Verification by Comparison of Assembly Calculations to Monte Carlo Results

Scott Palmtag
Core Physics Inc.

March 31, 2016

U.S. DEPARTMENT OF ENERGY | Nuclear Energy

REVISION LOG

Revision	Date	Affected Pages	Revision Description
0	03/31/2016	All	Initial Release

Document pages that are:

Export Controlled _____None_____

IP/Proprietary/NDA Controlled_____None_____

Sensitive Controlled_____None_____

Requested Distribution:

To:

Copy:

CONTENTS

CONTENTS iii

FIGURES iv

TABLES v

ACRONYMS vi

1. Introduction 1

2. Problem Geometry 1

3. MCNP Details 7

4. MPACT Details 8

5. MPACT Mesh Sensitivity 9

6. Results 12

7. Conclusion 17

8. References 18

Appendix A – Number Densities 19

FIGURES

Figure 2-1: CE 16x16 fuel assembly geometry with large water rods (lower right quadrant) 3

Figure 2-2: Krsko Westinghouse 16x16 fuel assembly geometry (no symmetry) 3

Figure 2-3: Surry Westinghouse 15x15 fuel assembly geometry (lower right quadrant).....4

Figure 2-4: TMI B&W 15x15 fuel assembly geometry with four gad rods (lower right quadrant).....4

Figure 2-5: Watts Bar 2A 17x17 fuel assembly geometry (lower right quadrant) 5

Figure 2-6: Watts Bar 2O fuel assembly geometry with 12 gad rods (lower right quadrant) 5

Figure 2-7: Watts Bar 2P fuel assembly geometry with 24 gad rods (lower right quadrant).....6

Figure 2-8: Watts Bar 2X fuel assembly geometry with thermal expansion and zoned enrichment (lower right quadrant) 6

Figure 6-1: Eigenvalue Differences (pcm) (all cases) 15

Figure 6-2: Eigenvalue Differences (pcm) (hot cases only) 15

Figure 6-3: Eigenvalue Differences (pcm) (cold cases only) 16

TABLES

Table 2-1: Assembly Geometry Descriptions 1

Table 2-2: Assembly Dimensions (cm) 2

Table 2-3: Coolant Densities 7

Table 4-1: MPACT Mesh Parameters 8

Table 5-1: Eigenvalue differences compared to default ray spacing (pcm) 9

Table 5-2: Eigenvalues differences compared to default polar angles (pcm) 10

Table 5-3: Eigenvalues differences compared to default azimuthal angles (pcm) 10

Table 6-1: Eigenvalue and Pin Power Results 12

Table 6-2: Hot Eigenvalue and Pin Power Differences by Parameter Subgroup 13

Table 6-3: Cold Eigenvalue and Pin Power Differences by Parameter Subgroup 14

ACRONYMS

BWR	boiling water reactor
CASL	Consortium for Advanced Simulation of Light Water Reactors
CE	Combustion Engineering
CZP	Cold Zero Power
GT	guide tube
HFP	Hot Full Power
HZP	Hot Zero Power
IT	instrument tube
LWR	light water reactor
PCM	percent mille (10^{-5})
PWR	pressurized water reactor
V&V	verification and validation
VERA	Virtual Environment for Reactor Applications

1. INTRODUCTION

This report summarizes the comparison of MPACT to MCNP for a variety of PWR assembly problems. The purpose of this study is to validate the MPACT multigroup library versus the continuous-energy Monte Carlo results contained in MCNP. This study is a companion study to the PWR pincell study reported in [1].

Additional comparisons to MCNP have been performed in [2] to validate the MPACT geometry. Reference [2] includes MCNP models of pincells, assemblies, and 3D configurations. The purpose of this report is to validate the MPACT cross section library at the many different statepoint conditions encountered in a reactor.

Fourteen different PWR assembly geometries are examined, including 15x15, 16x16, and 17x17 designs by different fuel vendors. The complete set of assembly geometries is listed in Table 2-1.

Each assembly geometry was run at 90 different statepoints, including:

- Three U-235 enrichments (2.1%, 3.1%, and 4.1%)
- Three hot coolant densities corresponding to typical inlet, average, and outlet conditions
- Three hot fuel temperatures (600, 900, and 1200K)
- One cold case at standard room temperature and density
- Three boron concentrations (0, 600, and 1300 ppm)

There are a total of 81 hot cases (3x3x3x3) and 9 cold cases (3x3) per assembly, for a total of 1260 cases total.

2. PROBLEM GEOMETRY

The fourteen assembly geometries modeled are listed in Table 2-1.

Table 2-1: Assembly Geometry Descriptions

Geometry	Description	Reference
ce16	CE 16x16 Assembly with large water rods	[3]
krsko	Krško Westinghouse 16x16	[4]
surry	Surry Westinghouse 15x15	[5]
tmi1	TMI B&W 15x15 with 4 gad rods	[6]
tmi2	TMI B&W 15x15 with no gad	[6]
wb2a	Watts Bar 2A 17x17	[7]
wb2e	Watts Bar 2E 17x17 12 Pyrex	[7]
wb2f	Watts Bar 2F 17x17 24 Pyrex	[7]
wb2l	Watts Bar 2L 17x17 80 IFBA rods	[7]
wb2m	Watts Bar 2M 17x17 128 IFBA rods	[7]
wb2o	Watts Bar 2O 17x17 12 gad rods	[7]
wb2p	Watts Bar 2P 17x17 24 gad rods	[7]
wb2w	Watts Bar 2W 17x17 thermally expanded	[7]*
wb2x	Watts Bar 2X 17x17 thermally expanded + zone enrichment	[7]*

The Watts Bar assemblies are slightly modified from [7]. The modifications include:

- The cladding material is natural zirconium to reduce the number of isotopes in the MCNP model,
- The enrichment, boron, fuel temperatures, and moderator densities are set by the case matrix (described below), and
- The moderator density inside the guide tubes (GT) and instrument tube (IT) are set to the core inlet conditions.

The assemblies "wb2w" and "wb2x" do not exist in [7]. These assemblies are the same as "wb2a" except that the dimensions have been thermally expanded, and "wb2x" has zoned enrichment rods. The thermally expanded dimensions have increased the rod radii, pin pitch, and assembly gaps. The material densities have not been decreased in the thermally expanded cases.

The assembly geometry descriptions are given in Table 2-2. These dimensions have been obtained from references [3-7]. Diagrams of selected assemblies are shown in Figures 2-1 to 2-8.

Table 2-2: Assembly Dimensions (cm)

			Fuel Rod			Guide Tube		Instrument Tube	
	ppitch	apitch	Rfuel	Rgap	Rclad	Rin	Rout	Rin	Rout
ce16	1.28524	20.64	0.41339	0.42164	0.48514	1.143	1.2446	1.143	1.2446
krsko	1.232	19.718	0.40960	0.41800	0.47500	0.5525	0.598	0.5525	0.598
surry	1.43	21.5036	0.46469	0.47422	0.53594	0.61392	0.69012	0.61392	0.69012
tmi1	1.4427	21.811	0.46950	0.47880	0.54610	0.63245	0.6731	0.56005	0.6261
tmi2	1.4427	21.811	0.46950	0.47880	0.54610	0.63245	0.6731	0.56005	0.6261
wb2a	1.26	21.5	0.40960	0.41800	0.47500	0.561	0.602	0.559	0.605
wb2e	1.26	21.5	0.40960	0.41800	0.47500	0.561	0.602	0.559	0.605
wb2f	1.26	21.5	0.40960	0.41800	0.47500	0.561	0.602	0.559	0.605
wb2l	1.26	21.5	0.40960	0.41800	0.47500	0.561	0.602	0.559	0.605
wb2m	1.26	21.5	0.40960	0.41800	0.47500	0.561	0.602	0.559	0.605
wb2o	1.26	21.5	0.40960	0.41800	0.47500	0.561	0.602	0.559	0.605
wb2p	1.26	21.5	0.40960	0.41800	0.47500	0.561	0.602	0.559	0.605
wb2w	1.2626	21.605	0.41208	0.41894	0.47607	0.56226	0.60335	0.56226	0.60335
wb2x	1.2626	21.605	0.41208	0.41894	0.47607	0.56226	0.60335	0.56226	0.60335

All non-gad fuel have a stack density of 10.257 g/cc and the main U-235 enrichments are 2.1, 3.1, and 4.1%. In addition, case "wb2x" uses U-235 enrichments of 1.6, 2.6, and 3.6% in the corner rods (corner rods are 0.5% lower than main enrichment).

All assemblies except "krsko" are octant symmetric and are run with quarter-symmetry in both MPACT and MCNP. The "krsko" assemblies do not exhibit any symmetry, and the full assembly is modeled in both codes.

The number densities for all materials are given in Appendix A.

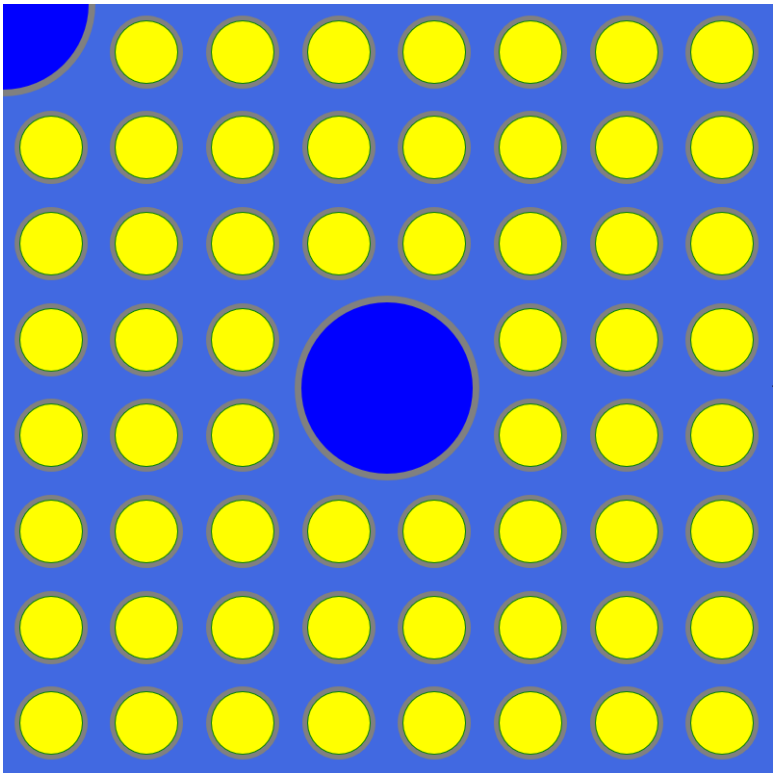

Figure 2-1: CE 16x16 fuel assembly geometry with large water rods (lower right quadrant)

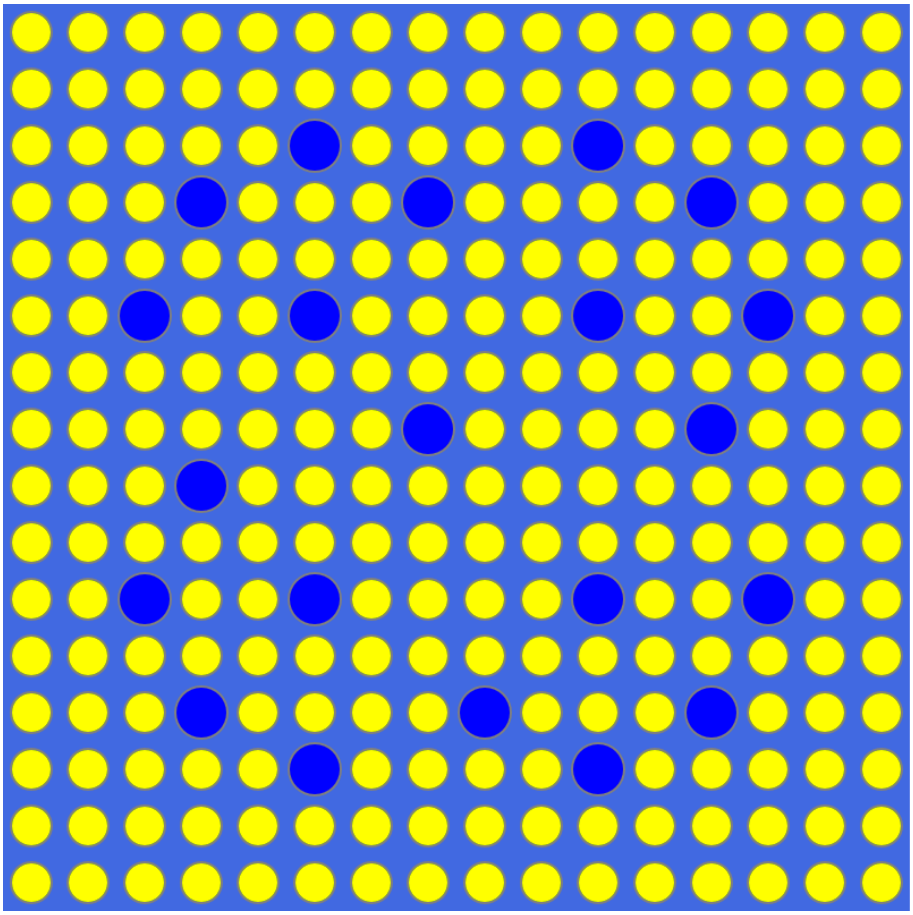

Figure 2-2: Krsko Westinghouse 16x16 fuel assembly geometry (no symmetry)

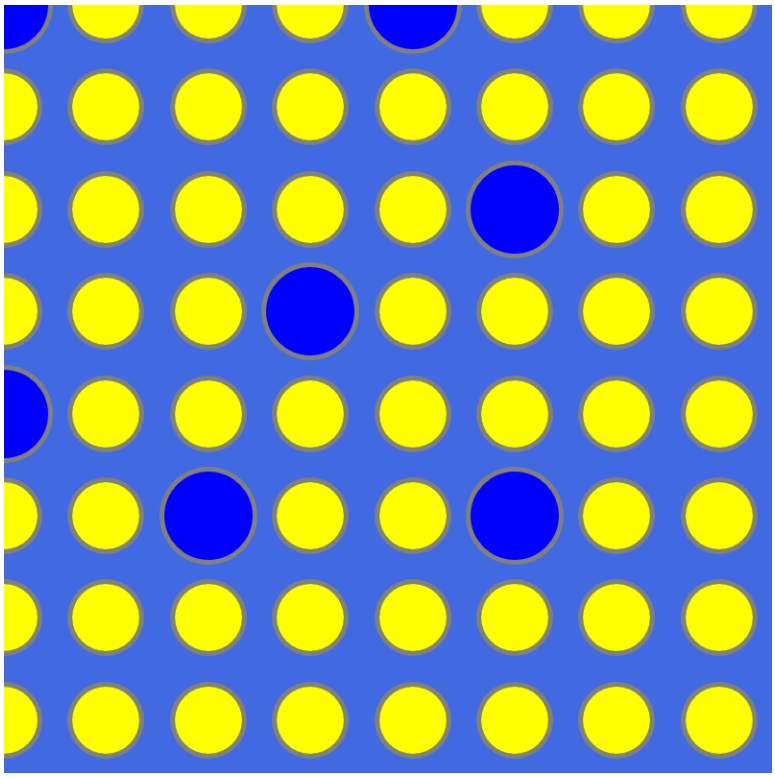

Figure 2-3: Surry Westinghouse 15x15 fuel assembly geometry (lower right quadrant)

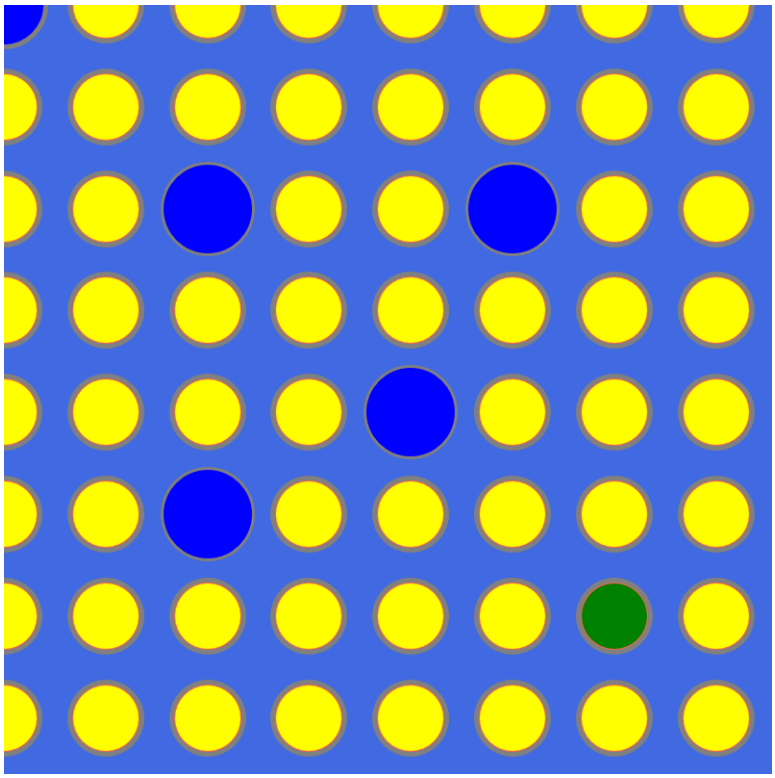

Figure 2-4: TMI B&W 15x15 fuel assembly geometry with four gad rods (lower right quadrant)

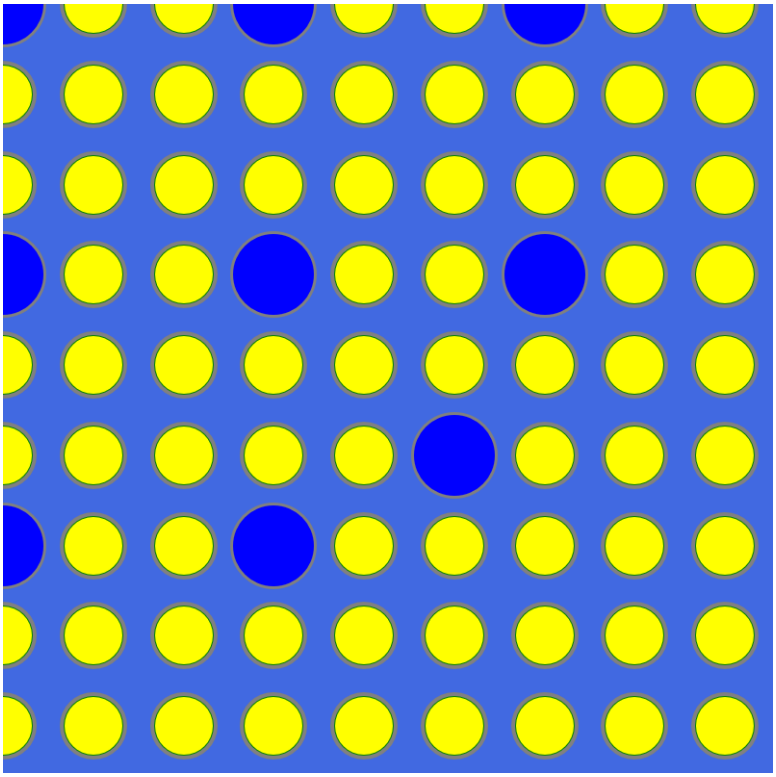

Figure 2-5: Watts Bar 2A 17x17 fuel assembly geometry (lower right quadrant)

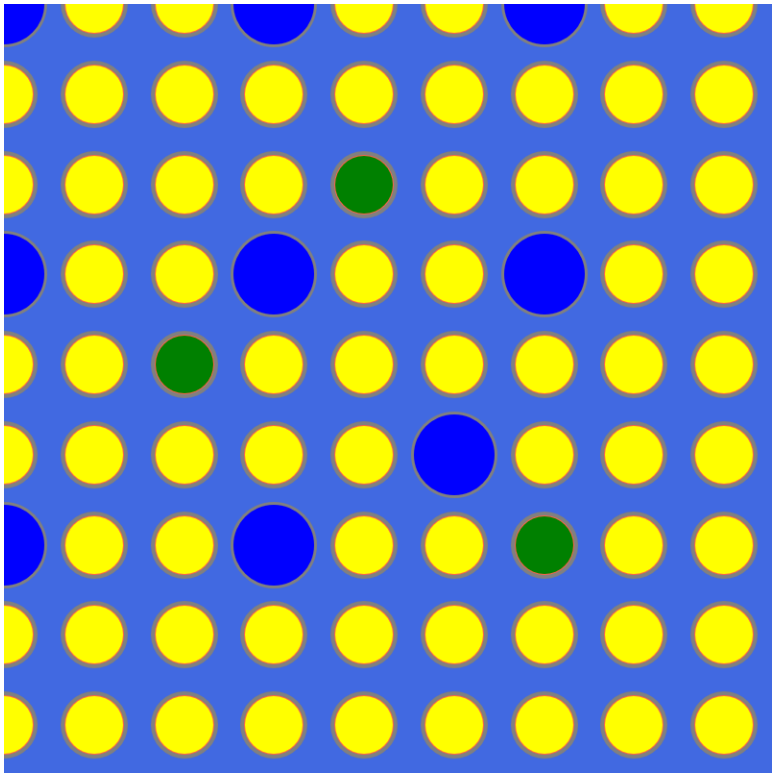

Figure 2-6: Watts Bar 2O fuel assembly geometry with 12 gad rods (lower right quadrant)

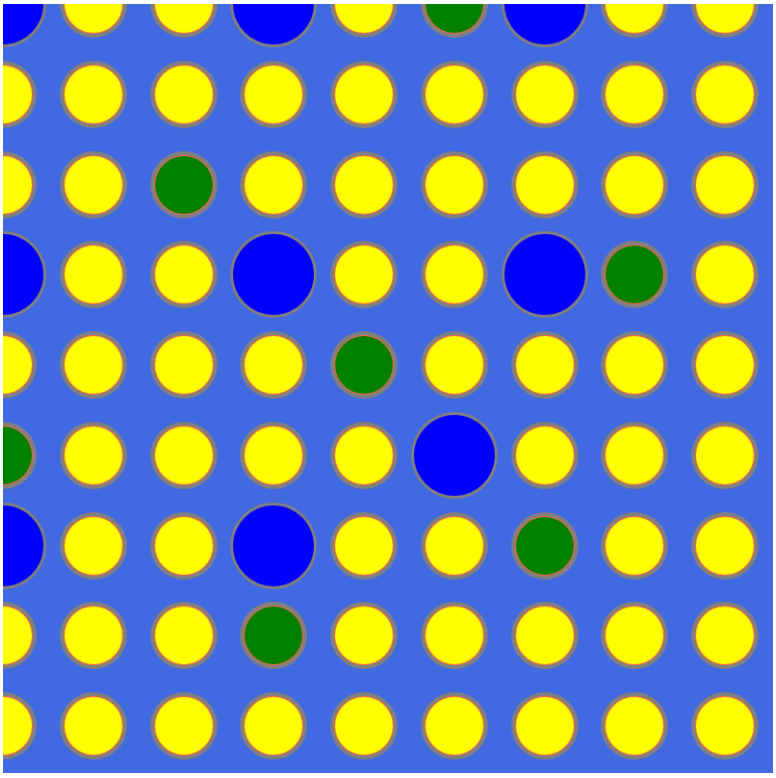

Figure 2-7: Watts Bar 2P fuel assembly geometry with 24 gad rods (lower right quadrant)

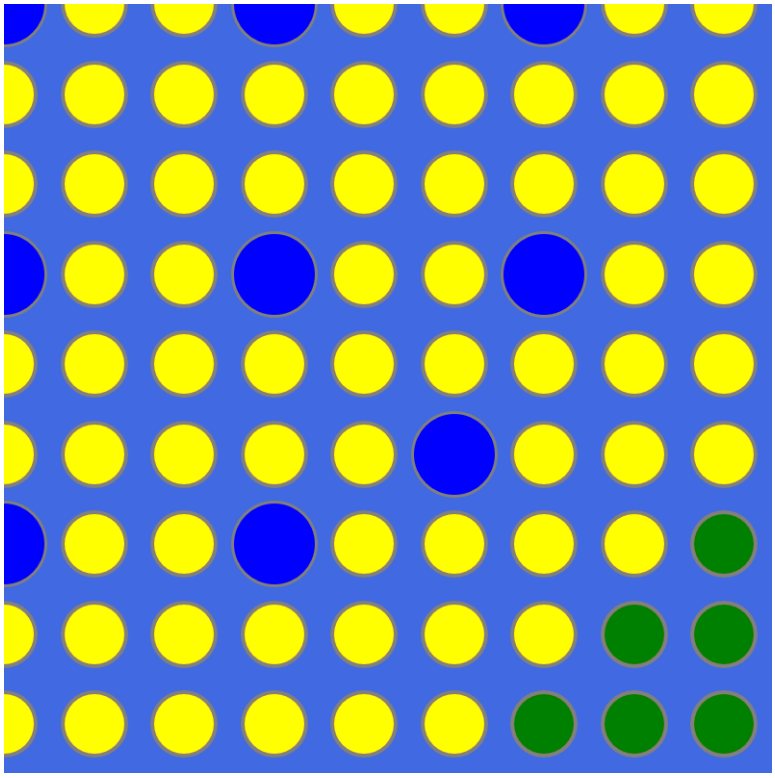

Figure 2-8: Watts Bar 2X fuel assembly geometry with thermal expansion and zoned enrichment (lower right quadrant)

The moderator densities correspond to typical PWR conditions at the core inlet, core average, and core outlet. The hot densities are calculated from subcooled steam tables at 2250 psia. The cold density is calculated at standard room conditions. The densities are listed in Table 2-3.

For cold cases, the moderator in the GT and IT is set to the cold density (den0). For all hot cases, the moderator in the GT and IT is always set to the core inlet density (den1).

Table 2-3: Coolant Densities

Reactor Condition	Nomenclature	Temperature (K)	Density (g/cc)
Cold	den0	293.6	1.0
Hot Inlet	den1	566.0	0.740816
Hot Average	den2	583.9	0.703158
Hot Outlet	den3	601.7	0.655986

All of the hot temperatures, except for the fuel, are set to 600K. These temperatures are higher than normal PWR conditions, but allow the use of the cross section libraries distributed with MCNP. In the future, we could generate MCNP libraries at 560K, and re-run the calculations, but it should not have a large impact on code-to-code comparisons. The hot fuel temperatures are either 600K, 900K, or 1200K, depending on the statepoint values.

All of the cold temperatures are set to 293.6K, which corresponds to one of the temperatures on cross section libraries distributed with MCNP.

3. MCNP DETAILS

MCNP is a general geometry, continuous energy Monte Carlo transport code developed by Los Alamos National Laboratory.

The version of MCNP used was MCNP 6.1.1b with ENDF/B VII.1 cross sections. The executable and cross sections used are the same ones distributed with MCNP. All of the MCNP cases were run on the ORNL Fission-4 Linux cluster.

For each case, MCNP was run with 200k neutrons per cycle, and 2000 active cycles, for a total of a total of 400M active particles per calculation. An additional 100 inactive cycles were also run to initialize the source distribution. The standard deviation on all eigenvalue results is between 2-3 pcm. The eigenvalue uncertainty in the MCNP calculation is lower than the typical differences observed between MCNP and MPACT and can effectively be ignored in the comparisons.

Except for the Krško assemblies, the largest uncertainty in the pin powers is 0.04%. The Krško assemblies were run with full symmetry, and therefore have a larger maximum pin power tally uncertainty of 0.08%. These uncertainties are very low compared to the differences between MCNP and MPACT and can effectively be ignored in the comparisons.

All of the material number densities were calculated by the MPACT material processing routines, and then copied to MCNP to maintain consistency between the codes.

4. MPACT DETAILS

MPACT version 2.1.0 was used built from the current source on March 28, 2016 (SHA1 7a6018e).

The cross section library was "`mpact47g_71s_v4.1m3_03192015.fmt`", which is based on ENDF/B-VII.1 cross section data. Subgroup cross sections were used in all the MPACT cases and all cross sections were P0 transport corrected (TCP0).

Default mesh parameters were used in MPACT, except for cases with IFBA. The default mesh parameters are shown in Table 4-1. A smaller ray spacing of 0.001 was used for all IFBA cases.

Table 4-1: MPACT Mesh Parameters

	Default Value
ray_spacing	0.05[1]
polars_octant	2
azimuthals_octant	16

[1]IFBA cases used a ray spacing of 0.001

All MPACT cases use the Chebyshev-Yamamoto quadrature set.

5. MPACT MESH SENSITIVITY

In this section, a sensitivity study was performed to evaluate the default mesh parameters used in MPACT.

A typical statepoint was selected for each assembly geometry (3.1% enrichment, 600 ppm boron, average density, and 900K fuel temperature) and a set of cases was run with different ray spacing, polar angles, and azimuthal angles. The results are compared to the default case to determine how converged the mesh is.

The results from decreasing the ray spacing are shown in Table 5-1. The default ray spacing is 0.05, but the IFBA cases "wb2l" and "wb2m" are run with a ray spacing of 0.001. (The IFBA results are shaded in green below).

Table 5-1: Eigenvalue differences compared to default ray spacing (pcm)

	ray 0.04	ray 0.02	ray 0.01	ray 0.005	ray 0.001
ce16	-6.1	-5.5	-5.5	-5.4	-5.4
krsko	-16.6	-12.9	-12.7	-13.9	-13.9
surry	-1.4	-0.5	-1.1	-1.2	-1.1
tmi1	13.3	-3.6	-8.3	-7.9	-8.0
tmi2	1.2	-0.4	-1.2	-1.0	-1.1
wb2a	0.1	-0.6	-1.2	-0.9	-1.1
wb2e	-1.2	-0.2	-0.8	-0.4	-1.0
wb2f	-8.3	-6.9	-5.8	-6.3	-6.7
wb2l	-78.5	-32.1	59.0	152.0	203.3
wb2m	-116.2	-34.6	85.7	198.1	284.0
wb2o	2.1	-6.4	-15.6	-8.7	-13.5
wb2p	2.8	17.1	0.2	5.5	3.5
wb2w	-3.2	-1.5	-1.6	-1.8	-1.9
wb2x	-3.2	-1.6	-1.6	-1.8	-1.9

The results of running with three polar angles is shown in Table 5-2. The default option is two polar angles, and three polar angles is the highest number of angles available with the Chebyshev-Yamamoto quadrature set.

Table 5-2: Eigenvalues differences compared to default polar angles (pcm)

	polar3
ce16	39.9
krsko	45.8
surry	39.8
tmi1	37.1
tmi2	40.6
wb2a	41.0
wb2e	36.3
wb2f	31.8
wb2l	42.7
wb2m	43.5
wb2o	30.4
wb2p	21.9
wb2w	41.0
wb2x	40.8

The results of running with increased number of azimuthal angles is shown in Table 5-3. The default number of azimuthal angles is 16. There are several blank spots in this table where the code has trouble converging. This issue is currently being investigated, but the initial thoughts are that the ray spacing is too coarse for the increased number of angles and we are getting duplicate angles in the solution.

Table 5-3: Eigenvalues differences compared to default azimuthal angles (pcm)

	azi 32	azi 64	azi 128
ce16	37.8	53.3	
krsko	19.6	39.5	40.4
surry	38.5	46.4	49.0
tmi1	29.5		
tmi2	35.5		
wb2a	43.0	56.6	58.3
wb2e	41.6	60.2	
wb2f	38.1		
wb2l	65.3	49.6	
wb2m	50.1		
wb2o	41.6	51.6	54.1
wb2p	50.9		73.8
wb2w	38.8	51.3	
wb2x	38.7	51.3	

Based on these results, the default mesh is converged in ray spacing to less than 20 pcm. The default polar angle selection is approximately 40 pcm low, and the default number of azimuthal angles is about 50 pcm low.

The selection of the default mesh must be made while considering the overall uncertainty in the problem and run-times. Having a mesh converged to less than 100 pcm is reasonable for our cases.

If a tighter mesh is desired, it is recommended that the number of polar angles be increased to 3, and the number of azimuthal angles be increased to 32.

6. RESULTS

A summary of the eigenvalue and pin power results is given in Table 6-1. Results are shown for all cases and for the hot and cold cases separately. There are 1260 total cases, of which 1134 are hot and 126 are cold.

The differences between the MCNP and MPACT eigenvalues are in "pcm", and defined as:

$$\text{Diff} = (k_{\text{MPACT}} - k_{\text{MCNP}}) \times 10^5 \text{ pcm}$$

The pin powers have been normalized such that the average pin power is equal to 1.0 in each assembly. The pin power difference for a single pin "i" are then defined as:

$$\text{Diff}^i = \left(P^i_{MPACT} - P^i_{MCNP}\right) \times 100\%$$

The RMS pin power differences is then

$$RMS = \sqrt{\frac{1}{N}\sum_{i=1}^{N}(P^i_{MPACT} - P^i_{MCNP})} \times 100\%$$

The RMS value is closely related to the standard deviation since the average error is zero, due to the choice of normalization.

The average RMS "AveRMS" is the average RMS value over all assemblies.

The maximum pin difference "MaxPin" is the maximum pin difference over all assemblies.

Table 6-1: Eigenvalue and Pin Power Results

	Ave (pcm)	Sdev (pcm)	Min (pcm)	Max (pcm)	AveRMS (%)	MaxPin (%)	Count
All	21.6	103.3	-432.9	287.2	0.13	0.97	1260
Hot	40.2	84.6	-168.0	287.2	0.11	0.53	1134
Cold	-145.5	106.7	-432.9	22.0	0.25	0.97	126

Overall, the eigenvalue results are acceptable. The average of all 1134 hot cases is 40.2 pcm with a standard deviation of 84.6 pcm. All of the hot cases are between -168 and +288 pcm. A reasonable goal is to have all eigenvalue differences between +/- 200 pcm. The cold cases have an approximately -200 pcm bias compared to the hot cases, and a larger standard deviation.

The hot pin power results look very good. Almost all of the hot assemblies have a maximum pin power less than 0.5%. The only assemblies with a maximum pin power greater than 0.5% is the high gad cases "wb2o". The cold pin power results are not as good, and the maximum error is almost 1%.

It is suggested that additional investigation be done to determine the cause of the large cold bias and large cold pin power errors.

Table 6-2 shows the hot results averaged over individual parameter subgroups (type, enrichment, boron, moderator density, and fuel temperature). A "subgroup" is defined as all the cases that have a particular parameter. For example, out of 1134 total hot cases, 378 cases have a boron concentration of 0ppm. Looking at the averages over subgroups allows us to identify "trends" in parameters.

Table 6-2: Hot Eigenvalue and Pin Power Differences by Parameter Subgroup

		Ave (pcm)	Sdev (pcm)	Min (pcm)	Max (pcm)	AveRMS (%)	MaxPin (%)	Count
Type	ce16	9.9	53.3	-108.3	119.4	0.11	0.28	81
Type	krsko	59.5	55.9	-68.4	168.8	0.11	0.43	81
Type	surry	-37.5	54.1	-164.6	61.9	0.09	0.25	81
Type	tmi1	9.7	53.6	-108.7	125.9	0.15	0.49	81
Type	tmi2	-36.0	55.2	-168.0	67.9	0.10	0.28	81
Type	wb2a	10.5	54.2	-120.8	117.7	0.10	0.26	81
Type	wb2e	101.8	46.4	-7.8	192.3	0.06	0.20	81
Type	wb2f	162.5	40.1	68.2	238.9	0.11	0.33	81
Type	wb2l	-11.8	32.9	-97.6	43.2	0.12	0.32	81
Type	wb2m	-17.4	27.4	-85.5	30.9	0.12	0.32	81
Type	wb2o	118.5	55.7	-2.1	243.5	0.17	0.43	81
Type	wb2p	173.3	51.6	48.8	287.2	0.20	0.53	81
Type	wb2w	9.9	55.1	-120.6	121.6	0.09	0.25	81
Type	wb2x	9.6	53.7	-113.7	120.3	0.08	0.25	81
Enrich	21	67.7	79.1	-65.4	287.2	0.11	0.52	378
Enrich	31	43.6	81.8	-120.0	255.8	0.11	0.53	378
Enrich	41	9.2	82.5	-168.0	217.3	0.12	0.51	378
Boron	0	45.6	94.6	-168.0	287.2	0.12	0.52	378
Boron	600	39.5	84.0	-159.4	249.2	0.11	0.51	378
Boron	1300	35.5	73.7	-133.3	215.3	0.11	0.53	378
Density	den1	23.3	80.3	-168.0	239.2	0.12	0.52	378
Density	den2	38.1	83.2	-158.4	259.4	0.11	0.53	378
Density	den3	59.2	86.5	-139.5	287.2	0.11	0.52	378
Tfuel	600	77.4	71.3	-38.3	287.2	0.12	0.53	378
Tfuel	900	52.3	75.4	-84.1	282.1	0.11	0.52	378
Tfuel	1200	-9.2	82.1	-168.0	238.6	0.11	0.51	378

Using a criteria of 100 pcm between subgroup differences to define a trend, there are no trends in enrichment, boron, density, or fuel temperature. There are trends in geometry type, and it appears that pyrex (wb2e and wb2f) and gad assemblies (wb2o and wb2p) have larger eigenvalue differences.

Only the wb2p assemblies have a maximum pin power difference over 0.5%.

Table 6-3 shows the cold results averaged over individual parameter subgroups. There is an approximate -200 pcm bias between hot and cold cases. Cold cases also show a trend in enrichment, which can help explain some of our cold critical results.

The largest cold pin power differences are in the "ce16" assemblies, which have the large water rods.

Table 6-3: Cold Eigenvalue and Pin Power Differences by Parameter Subgroup

		Ave (pcm)	Sdev (pcm)	Min (pcm)	Max (pcm)	AveRMS (%)	MaxPin (%)	Count
Type	ce16	-18.2	45.5	-108.9	22.0	0.32	0.97	9
Type	krsko	-52.1	42.7	-141.8	-8.1	0.25	0.71	9
Type	surry	-67.8	36.8	-142.1	-35.1	0.26	0.48	9
Type	tmi1	-109.7	43.0	-171.9	-60.4	0.28	0.58	9
Type	tmi2	-72.5	35.9	-145.8	-38.5	0.25	0.55	9
Type	wb2a	-82.2	46.3	-176.3	-35.6	0.23	0.46	9
Type	wb2e	-184.7	59.1	-261.5	-121.5	0.21	0.57	9
Type	wb2f	-220.7	71.6	-333.8	-138.9	0.20	0.75	9
Type	wb2l	-257.9	65.4	-367.7	-174.7	0.21	0.64	9
Type	wb2m	-307.5	68.9	-432.9	-212.8	0.17	0.56	9
Type	wb2o	-211.0	61.9	-308.0	-141.0	0.29	0.66	9
Type	wb2p	-287.0	80.0	-430.8	-189.2	0.34	0.84	9
Type	wb2w	-81.3	47.3	-175.6	-32.3	0.22	0.44	9
Type	wb2x	-84.7	49.4	-183.6	-32.7	0.21	0.43	9
Enrich	21	-205.5	115.4	-432.9	-24.1	0.24	0.81	42
Enrich	31	-131.2	95.7	-340.7	17.3	0.25	0.88	42
Enrich	41	-99.9	78.8	-280.8	22.0	0.26	0.97	42
Boron	0	-141.8	127.8	-432.9	20.8	0.27	0.97	42
Boron	600	-146.1	104.3	-375.4	22.0	0.25	0.81	42
Boron	1300	-148.7	86.4	-328.8	10.8	0.22	0.73	42

The eigenvalue results over all cases is shown as a histogram in Figure 6-1. A histogram of only the hot cases is shown in Figure 6-2, and a histogram of only the cold cases is shown in Figure 6.3. The cold eigenvalue differences do not appear to have a "Normal" shape to them, which usually indicates non-random trends in the data.

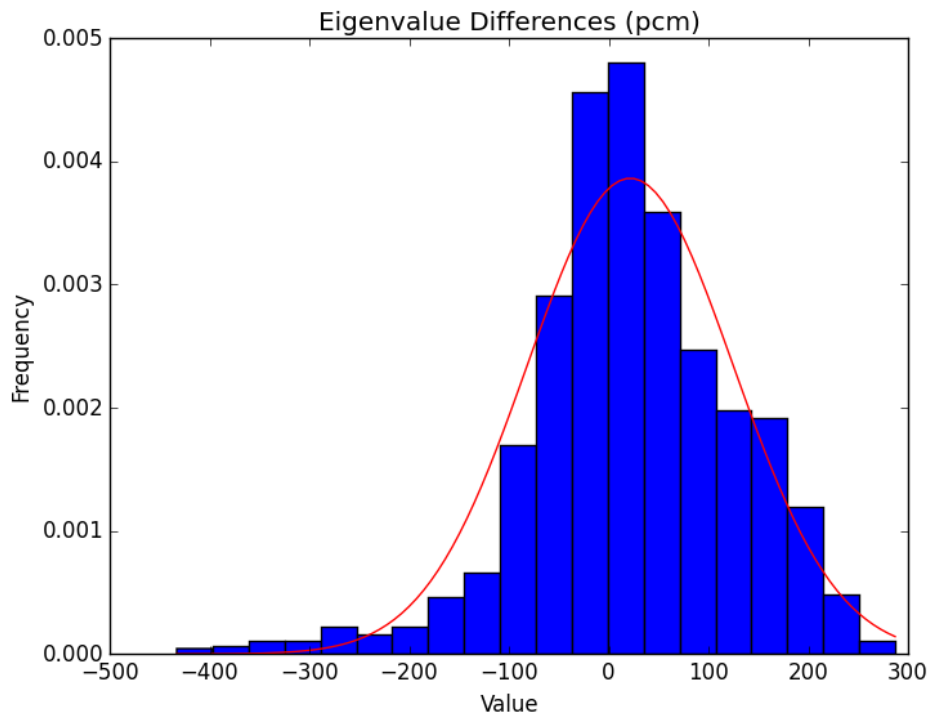

Figure 6-1: Eigenvalue Differences (pcm) (all cases)

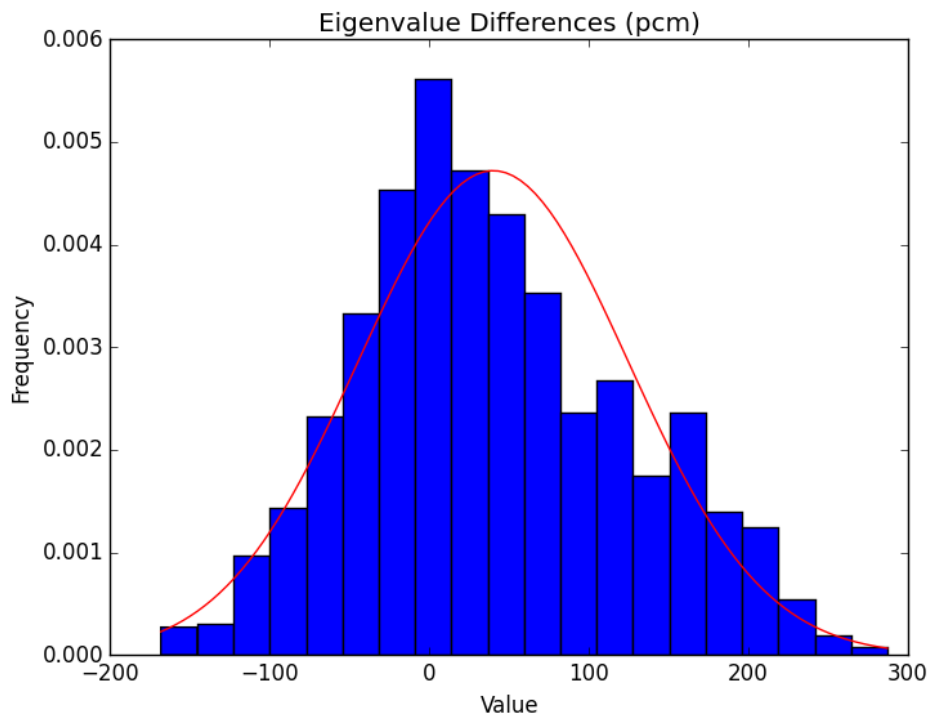

Figure 6-2: Eigenvalue Differences (pcm) (hot cases only)

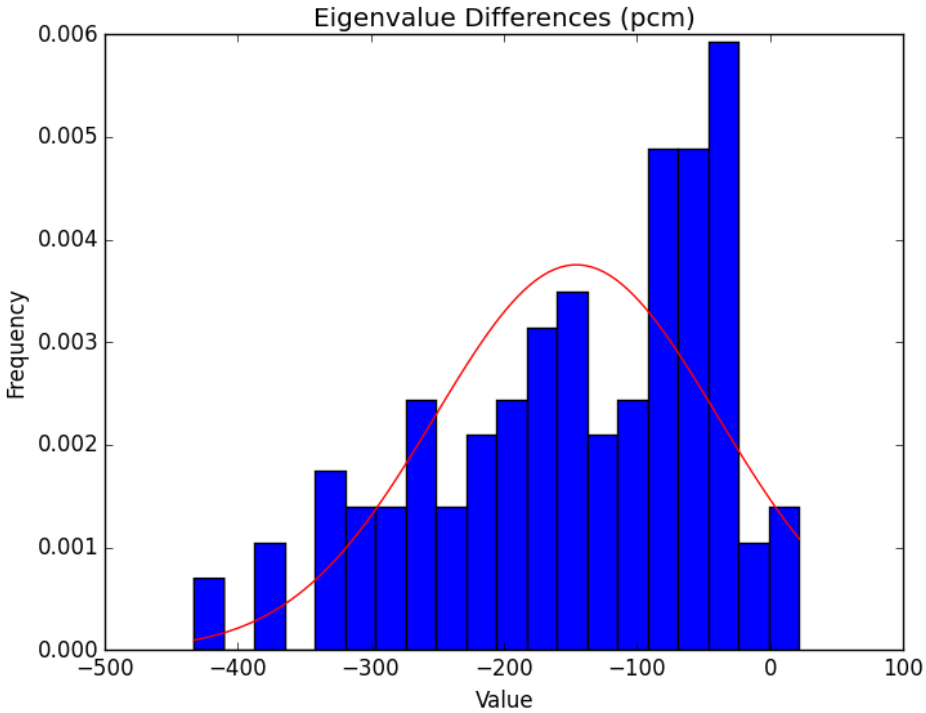

Figure 6-3: Eigenvalue Differences (pcm) (cold cases only)

7. CONCLUSION

In this study, a large number of assembly comparisons were made between MPACT and MCNP to validate the MPACT multigroup library over a range of conditions typically found in an operating PWR. The comparisons cover a total of 14 assembly geometries run at 90 statepoints each.

The average eigenvalue difference between MPACT and MCNP eigenvalues is 21.6 pcm with a standard deviation of 103.3 pcm. The hot eigenvalues have a difference of 40.2 pcm with a standard deviation of 84.6 pcm. The cold eigenvalues have a large negative bias with and average difference of -145.5 pcm and standard deviation of 106.7 pcm.

The hot eigenvalue results are acceptable, but a reasonable goal should be to have all eigenvalue differences between +/- 200 pcm. The cold eigenvalues are not acceptable, and more investigation needs to be performed to improve the cold bias.

The hot pin power results are very good. The maximum pin power difference across all 1260 statepoints is 0.53%. The largest pin power difference occurs in the heavy gad assembly. All other assembly geometries are less than 0.5%. The cold pin powers are not as good, with a maximum error approaching 1%.

No trends have been observed in the hot results for enrichment, boron, density, or fuel temperature. However, the large absorber assemblies with pyrex and gad have larger eigenvalue differences than desired (average differences of 100-150 pcm instead of 20 pcm).

One important result of this report is that we now have a large suite of test cases to evaluate future cross section libraries. This test suite can be used in future development to evaluate any improvements in our library.

8. REFERENCES

[1] Palmtag, S., MPACT Library Verification by Comparison of Pincell Calculations to Monte Carlo Results, CASL Technical Report CASL-U-2015-0281-001, February 10, 2016.

[2] Gurecky, W., and Schneider, E., MCNP MCNPX and KENO-VI Simulations of WBNP Unit 1 with Keno Comparisons, CASL Technical Report CASL-U-2015-0221-000, February 20, 2015.

[3] Palo Verde Nuclear Generating Station Units 1, 2, and 3, Updated Final Safety Analysis Report (USAR), Chapter 4, Revision 14, June 2007. (NRC Document ML072250202)

[4] Krsko Updated Safety Analysis Report (USAR), Chapter 4, Revision 21.

[5] "Reactor Core Physics Design and Operating Data for Cycles 1, 2, and 3 of Surry unit 1 PWR Power Plant", EPRI Report NP-79-2-LD, March (1979)

[6] Ivanov, K, et al., "Benchmarks for uncertainty analysis in modelling (UAM) for the design, operation and safety analysis of LWRs, Volume I: Specification and Support Data for Neutronics Cases (Phase I)", Nuclear Energy Agency Report NEA/NSC/DOC(2013)7, May 30, 2013.

[7] Godfrey, A., VERA Core Physics Benchmark Progression Problem Specifications, Revision 4, CASL Technical Report: CASL-U-2012-0131-004, August 29, 2014.

APPENDIX A – NUMBER DENSITIES

The number densities for each material are given below (atoms/cc * 10^{24}).

Fuel (2.1% enrichment)

```
92234     4.019258513190756E-06
92235     4.864992501186317E-04
92236     2.228399660642638E-06
92238     2.238749037607419E-02
 8016     4.576032003944108E-02
```

Fuel (3.1% enrichment)

```
92234     6.129696313485968E-06
92235     7.181546463859156E-04
92236     3.289492367984266E-06
92238     2.215528646178965E-02
 8016     4.576549470430984E-02
```

Fuel (4.1% enrichment)

```
92234     8.298843086779618E-06
92235     9.498029937490817E-04
92236     4.350552787967713E-06
92238     2.192303162546796E-02
 8016     4.577067225771165E-02
```

Gap

```
 2004     2.648020953979913E-05
```

Clad (natural Zr)

```
40090     2.228100088688169E-02
40091     4.858928598362912E-03
40092     7.426969216182290E-03
40094     7.526569805645464E-03
40096     1.212565660696912E-03
```

Gad Fuel (1.4% + 2% gad) – used in TMI1 with 2.1% enrichment fuel

```
92234     2.510356612569076E-06
92235     3.143478494050798E-04
92236     1.439863762929150E-06
92238     2.185552833597460E-02
 8016     4.535898592203950E-02
64152     1.348226793853373E-06
64154     1.469543108099402E-05
64155     9.976671736968666E-05
64156     1.379886003364438E-04
64157     1.054969309213878E-04
64158     1.674467233070903E-04
64160     1.473589067710153E-04 / gad 2%
```

Gad Fuel (2.4% + 2% gad) – used in TMI1 with 3.1% enrichment fuel

```
92234     4.501992779940760E-06
92235     5.388738426003040E-04
92236     2.468300388308703E-06
92238     2.163052381584287E-02
 8016     4.536399885811290E-02
64152     1.348226793853373E-06
64154     1.469543108099402E-05
64155     9.976671736968666E-05
64156     1.379886003364438E-04
64157     1.054969309213878E-04
64158     1.674467233070903E-04
64160     1.473589067710153E-04 / gad 2%
```

Gad Fuel (3.4% + 2% gad) – used in TMI1 with 4.1% enrichment fuel

```
92234     6.566394531571118E-06
92235     7.633930074576481E-04
92236     3.496705736629121E-06
92238     2.140545431001251E-02
 8016     4.536901505613400E-02
64152     1.348226793853373E-06
64154     1.469543108099402E-05
64155     9.976671736968666E-05
64156     1.379886003364438E-04
64157     1.054969309213878E-04
64158     1.674467233070903E-04
64160     1.473589067710153E-04 / gad 2%
```

Gad Fuel (1.8% + 5% gad) – used with wb2o and wb2p

```
92234     3.184894429224019E-06
92235     3.905123044341210E-04
92236     1.788733459436102E-06
92238     2.103060525002554E-02
64152     3.359529864881016E-06
64154     3.661886363491889E-05
64155     2.486054020418233E-04
64156     3.438476931704493E-04
64157     2.628835567026993E-04
64158     4.172559469965151E-04
64160     3.671980522017794E-04
 8016     4.537244090256850E-02 / gad 5%
```

Fuel (1.6% enrichment) – used in wb2x zone enrichment with 2.1% fuel

```
92234     2.993401789425346E-06
92235     3.706689102551918E-04
92236     1.697841206583624E-06
92238     2.250356599892766E-02
 8016     4.575773400431383E-02 / 1.6%
```

Fuel (2.6% enrichment) – used in wb2x zone enrichment with 3.1% fuel

```
92234     5.065941944794528E-06
92235     6.023278290585090E-04
92236     2.758950048828028E-06
92238     2.227139596351662E-02
 8016     4.576290697593752E-02 / 2.6%
```

Fuel (3.6% enrichment) – used in wb2x zone enrichment with 4.1% fuel

```
92234     7.207954056557465E-06
92235     8.339797014759951E-04
92236     3.820026615249209E-06
92238     2.203916440084507E-02
 8016     4.576808314974187E-02 / 3.6%
```

Pyrex – used in wb2e and wb2f

```
 5010     9.607772283238149E-04
 5011     3.891622172497563E-03
 8016     4.666797616642821E-02
14000     1.968202004467158E-02 / pyrex-vera
```

Stainless Steel – used in wb2e and wb2f

```
 6000     3.208965159714260E-04
14000     1.715420303952830E-03
15031     6.999426637430164E-05
24050     7.649186869327455E-04
24052     1.475073422447215E-02
24053     1.672614798570479E-03
24054     4.163482832613400E-04
25055     1.753878317803186E-03
26054     3.447784576321783E-03
26056     5.412286235142948E-02
26057     1.249929271261278E-03
26058     1.663431021652268E-04
28058     5.308575803254905E-03
28060     2.044851924367664E-03
28061     8.888804443315597E-05
28062     2.834148364652267E-04
28064     7.217744738353442E-05 / ss
```

IFBA – used in wb2l and wb2m

```
40090     1.063198075262026E-02
40091     2.318568882898179E-03
40092     3.543978753811024E-03
40094     3.591505862467331E-03
40096     5.786084220932913E-04
 5010     2.164332764282830E-02
 5011     1.968449178012004E-02 / IFBA material
```

Coolant (4 densities and 3 boron concentrations)

Boron 0 ppm

```
1001     6.689001271791226E-02
8016     3.344500635895613E-02 / den0 0 ppm

1001     4.955319166163290E-02
8016     2.477659583081645E-02 / den1 0 ppm

1001     4.703424756270175E-02
8016     2.351712378135087E-02 / den2 0 ppm

1001     4.387891188277240E-02
8016     2.193945594138620E-02 / den3 0 ppm
```

Boron 600 ppm

```
1001     6.684987871028152E-02
8016     3.342493935514076E-02
5010     6.651027465151196E-06
5011     2.677122110344777E-05 / den0 600 ppm

1001     4.952345974663591E-02
8016     2.476172987331796E-02
5010     4.927187562623448E-06
5011     1.983254893297177E-05 / den1 600 ppm

1001     4.700602701416413E-02
8016     2.350301350708206E-02
5010     4.676723170340784E-06
5011     1.882439828865813E-05 / den2 600 ppm

1001     4.385258453564273E-02
8016     2.192629226782137E-02
5010     4.362980902754672E-06
5011     1.756154624676629E-05 / den3 600 ppm
```

Boron 13000 ppm

```
1001     6.680305570137898E-02
8016     3.340152785068949E-02
5010     1.441055950782759E-05
5011     5.800431239080351E-05 / den0 1300ppm

1001     4.948877251247277E-02
8016     2.474438625623639E-02
5010     1.067557305235081E-05
5011     4.297052268810550E-05 / den1 1300 ppm

1001     4.697310304087024E-02
8016     2.348655152043512E-02
5010     1.013290020240503E-05
5011     4.078619629209261E-05 / den2 1300 ppm

1001     4.382186929732479E-02
8016     2.191093464866240E-02
5010     9.453125289301790E-06
5011     3.805001686799363E-05 / den3 1300 ppm
```